

Full Paper

Study of Copper and Purine-Copper Complexes on Modified Carbon Electrodes by Cyclic and Elimination Voltammetry

Libuse Trnkova^{1,*}, Lenka Zerzankova¹, Filip Dycka¹, Radka Mikelova¹ and Frantisek Jelen²

1 Department of Chemistry, Faculty of Science, Masaryk University, Kotlarska 2, 611 37 Brno, Czech Republic

2 Institute of Biophysics, Academy of Sciences of the Czech Republic, v.v.i., Kralovopolska 135, Brno 612 65, Czech Republic

* Author to whom correspondence should be addressed; E-mail: libuse@chemi.muni.cz

Received: 30 December 2007 / Accepted: 15 January 2008 / Published: 24 January 2008

Abstract: Using a paraffin impregnated graphite electrode (PIGE) and mercury-modified pyrolytic graphite electrode with basal orientation (Hg-PGEb) copper(II) and Cu(II)-DNA purine base solutions have been studied by cyclic (CV) and linear sweep voltammetry (LSV) in connection with elimination voltammetry with linear scan (EVLS). In chloride and bromide solutions (pH 6), the redox process of Cu(II) proceeded on PIGE with two cathodic and two anodic potentially separated signals. According to the elimination function E4, the first cathodic peak corresponds to the reduction $\text{Cu(II)} + e^- \rightarrow \text{Cu(I)}$ with the possibility of fast disproportionation $2\text{Cu(I)} \rightarrow \text{Cu(II)} + \text{Cu(0)}$. The E4 of the second cathodic peak signaled an electrode process controlled by a surface reaction. The electrode system of Cu(II) on Hg-PGEb in borate buffer (pH 9.2) was characterized by one cathodic and one anodic peak. Anodic stripping voltammetry (ASV) on PIGE and cathodic stripping voltammetry (CSV) on Hg-PGEb were carried out at potentials where the reduction of copper ions took place and Cu(I)-purine complexes were formed. By using ASV and CSV in combination with EVLS, the sensitivity of Cu(I)-purine complex detection was enhanced relative to either ASV or CSV alone, resulting in higher peak currents of more than one order of magnitude. The statistical treatment of CE data was used to determine the reproducibility of measurements. Our results show that EVLS in connection with the stripping procedure is useful for both qualitative and quantitative microanalysis of purine derivatives and can also reveal details of studied electrode processes.

Keywords: Copper-purine complexes, Paraffin-impregnated graphite electrode, Mercury-film electrode, Anodic and cathodic stripping techniques, Elimination voltammetry, Confidence ellipse.

1. Introduction

Nucleic acid bases and some of their derivatives can be detected by stripping analysis with mercury electrodes. Using cathodic stripping voltammetry (CSV) in connection with cyclic voltammetry (CV) or differential pulse voltammetry (DPV), we were able to detect purine and pyrimidine bases at very low concentrations [1]. Voltammetric ultra-trace determination of some nucleic bases in the presence of Cu(II) using a mercury electrode or solid amalgam electrodes has been also described [2-6]. Determination is based on the formation of purine-copper complex at the electrode surface and subsequent stripping resulting in a voltammetric signal suitable for analytical purposes [3,7,8].

As mercury and amalgam electrodes are avoided for both industrial and scientific purposes in many countries around the world, new types of working electrodes for analysis of nucleic acids and their components are needed. Modified carbon electrodes are widely used in many applications in bioanalysis. A number of protocols describing modification of these electrodes have been published [9]. Recently, paraffin-impregnated carbon electrodes (PIGE) have been used for kinetic measurements [10-13] and for electrochemical studies where obtained data were evaluated by elimination voltammetry [14-17]. Electrochemical characteristics of PIGE electrodes are comparable with other carbon electrodes; their advantages include easy of preparation and very low negative potential limits [18].

The electrochemical oxidation of adenine and guanine and other purine derivatives at carbon electrodes have been reported [19-23]. Formation of complexes of these compounds with metals, including copper, has been studied extensively by electrochemical methods [3,7,24-26]. Species Cu(II) can be reduced to Cu(I) and in the presence of purines, such as adenine or guanine, Cu(I) reacts with purines to form insoluble compounds that accumulate on electrode surfaces [7,24]. This approach can be applied for the detection of oligodeoxynucleotide (ODN) after acid hydrolysis which releases purine bases from the ODN chain [6,27,28].

In this paper, elimination voltammetry with linear scan (EVLS) [29-32] in conjunction with an adsorptive stripping technique was used to detect two purine derivatives in the presence of copper(II). The measurements were carried out with two modified carbon electrodes: paraffin-impregnated graphite electrodes (PIGE) and mercury-modified pyrolytic graphite electrodes with basal orientation (Hg-PGEb). To understand the complex electrode processes we investigated redox behavior of Cu(II) salts at both electrodes.

2. Material and Methods

2.1. Chemicals

Chemicals purchased from Sigma-Aldrich were of ACS quality. The solutions contained CuCl_2 in NaCl or CuBr_2 in NaBr (pH 6.0) and CuSO_4 in 0.05 M sodium tetraborate (pH 9.2) for PIGE and Hg-PGEb, respectively, and were prepared using Millipore water (Direct-Q[®] 3 Ultrapure Water Systems). The pH was adjusted by 0.2 M NaOH and measured by means of pH meter CyberScan (Eutech Instruments, PC 5500) with Hamilton Single Pore Glass Electrode and temperature sensor Accumet.

2.2 Instrumentation

The voltammetric measurements were carried out with the AUTOLAB electrochemical system (Ecochemie, Utrecht, Netherlands) equipped with a potentiostat/galvanostat PGStat30. A three-electrode system was used. The working electrode was a paraffin-impregnated graphite electrode (PIGE) with an area of 12.56 mm^2 or a pyrolytic graphite electrode with basal orientation modified by a mercury layer (Hg-PGEb) with an area of 30 mm^2 . A platinum wire served as the counter electrode. The reference electrode was $\text{Ag}|\text{AgCl}||3 \text{ M KCl}$.

2.3 Preparation of graphite electrodes

The porous graphite cylinder was 150 mm long and 6 mm in diameter, mensural electric resistance was $1000 \mu\Omega/\text{cm}$, and porosity 30%. The electrode contained the following admixtures (ppm): B, 0.01; Ca, 0.1; Cu, 0.1; Fe, 0.2; Mg, 0.01; Si, 0.1; Al, 0.05; Ti, 0.01. The graphite rod was impregnated with paraffin to fill the pores and to suppress the background current [9,33,34]. The graphite was impregnated with paraffin at about 150–200 °C for 3 hours [35]. This procedure was applied at low pressure provided by an oil pump. The contact surface of the graphite electrode with the electrolyte was mechanically regenerated, cleaned, and washed by using abrasive paper (granularity of P1000), filter paper, and distilled water, prior to measurement. Before a measurement, solutions were deaerated by argon (99.996 vol. % purity) for 15 minutes. The basal oriented pyrolytic graphite rod was obtained from GE-Advance Ceramics. The surface of the pyrolytic graphite electrode with basal orientation (PGEb) was refreshed with adhesive tape without mechanical polishing and sonicated in triply distilled water (30 s). The electrodeposition of the mercury on PGEb surface was carried out in 30 mM $\text{Hg}(\text{NO}_3)_2$ solution using the potentiostat with a three-electrode system. The deposition potential was -1.2 V vs. $\text{Ag}|\text{AgCl}||3 \text{ M KCl}$. The thickness h of the mercury layer was controlled by a change of the deposition time t and current value I with respect to the Faraday law:

$$h = \frac{ItM}{n\rho AF} \quad (1)$$

where h is the thickness of the Hg film (cm), I the current, t the time of electrolysis, M the relative molar mass of Hg, n the number of electrons transferred, ρ the density of Hg (g/cm^3), A the area of the

electrode (cm^2), and F is the Faraday constant. The geometrical areas A of the Hg-PGEb were 0.3 cm^2 . Before measurements, the Hg-PGEb was repetitively scanned (20 cycles) in the potential region from 0 to -1.80 V in 0.05 M sodium tetraborate.

The GPES 4.9 Autolab software was used for measurements and for processing (smoothing) of recorded voltammetric curves and treatment of data.

2.4. Methods

2.4.1 Elimination voltammetry with linear scan

The elimination voltammetry with linear scan (EVLS), as a mathematical transformation of voltammetric curves, can be used to eliminate some chosen current components and to conserve the others. This transformation arises from the different dependence of partial current on scan rate and is based on the two presumptions [36]:

a) A total voltammetric current I can be given as a sum of particular currents I_j :

$$I = \sum_{j=1}^n I_j = I_d + I_c + I_k + \dots \quad (2)$$

where I_d , I_c , and I_k are the diffusion, charging, and kinetic currents, respectively;

b) A particular current I_j can be expressed as a product of two functions—potential function $Y_j(E)$ and scan rate function $W_j(\nu)$:

$$I_j = Y_j(E) \cdot W_j(\nu) \quad (3)$$

Based on the dependence of partial current on scan rate, equation (2) can be rewritten:

$$I = Y_d(E) \cdot \nu^{1/2} + Y_c(E) \cdot \nu^1 + Y_k(E) \cdot \nu^0 + \dots \quad (4)$$

Using an elimination function $f(I)$ containing a linear combination of two or three currents measured at two or three scan rates, the elimination procedure yields a new curve that allows deeper characterization of electrode processes and/or enhancement of CV or LSV responses. The theory of EVLS was published ten years ago and has been developed and improved with applications described in a number of published works [14,15,17,29,31,32,37-44]. It was found that the EVLS transformation E4 (conservation of the diffusion current and elimination of kinetic and charging currents, eq. 5) is very sensitive function not only in electroanalysis but also in the study of electrode processes. Even in the case of electroactive species adsorbed on electrode surfaces, the elimination function E4 yields a signal (peak-counterpeak) that increases substantially the sensitivity of voltammetric responses and allows separation of overlapped signals [31,32,39,41,43-45]. For the multiplayer 2, the elimination function E4 corresponds to the linear combination:

$$f(I) = -11,657 I_{v_{ref}/2} + 17,485 I_{v_{ref}} - 5,8284 I_{2v_{ref}} \quad (5)$$

where $I_{v_{ref}/2}$, $I_{v_{ref}}$, and $I_{2v_{ref}}$ are currents measured at half of reference scan rate, reference scan rate, and two times of reference scan rate, respectively. The theoretical EVLS curve for adsorbed electroactive species has been described in our previous publications [31,32,39,41]. From an experimental point of view, the EVLS procedure was carried out by recording three voltammetric curves at different scan rates; the other experimental parameters, such as potential step, potential range, and equilibrium time, were identical for all three scan rates. One of reference scan rates was chosen as the reference scan rate (v_{ref}) and elimination functions were calculated in Microsoft Excel with MACRA program for three polarization rates ($1/2v_{ref}$, v_{ref} , $2v_{ref}$).

2.4.2 Confidence ellipse

Method of a confidence ellipse (CE) was used for the statistical processing of measured data. Using CE procedure, multidimensional data such as cyclic voltammetric curves are transformed into two-dimensional data by Fourier Transformation (FT). Each curve can be expressed as a sum of chosen cosines and sinus functions:

$$F_k = \sum_{j=0}^{m-1} A_j \cos \frac{2\pi jk}{m} + i \sum_{j=0}^{m-1} A_j \sin \frac{2\pi jk}{m} \quad (6)$$

where A_j is amplitude of the curve at a particular point, m is total number of points which determines the curve, and the parameter k can take values from 0 to m [46]. The curve determined by m points with amplitude A is transformed into coordinates xf_k and yf_k . When curves are similar and differ from each other only by the multiplication factor, then the curves with coefficient $k=1$ are important and determine the character of the curve. For the first coefficient in FT the transformed curve is represented by a single point with coordinates xf_1 and yf_1 (i.e., $F_1 = xf_1 + iyf_1$) and from n voltammetric curves we obtain n points. Using orthogonal regression, these points are linked by a line with the slope b_T :

$$b_T = \frac{S_y - S_x}{2S_{xy}} \pm \sqrt{1 + \left(\frac{S_y - S_x}{2S_{xy}} \right)^2} \quad (7)$$

where $S_x = \sum x_c^2$, $S_y = \sum y_c^2$, $S_{xy} = \sum x_c y_c$ and $x_c = x_i - \bar{x}$; $y_c = y_i - \bar{y}$. The set of points is rotated to bring the regression line into the horizontal position (i.e., the x-axis). New coordinates of points are now x_r and y_r .

$$\begin{bmatrix} x_r & y_r \end{bmatrix} = \begin{bmatrix} x_c & y_c \end{bmatrix} \begin{bmatrix} \cos(\varphi) & -\sin(\varphi) \\ \sin(\varphi) & \cos(\varphi) \end{bmatrix}$$

where $\varphi = \text{tg}(b_T)$. The points are surrounded by 95% (99%) confidence ellipses, thus the half axes are twice (three) times the standard deviations Standard Error of Estimate Longitudinal (SEEL) and Standard Error of Estimate Transverse (SEET):

$$SEEL = (P + M) / 2$$

$$SEET = (P - M) / 2$$

$$P = \sqrt{\frac{(S_x + S_y + 2\sqrt{S_x S_y - S_{xy}^2})}{(n-1)}} \quad M = \sqrt{\frac{(S_x + S_y - 2\sqrt{S_x S_y - S_{xy}^2})}{(n-1)}} \quad (8)$$

A backward rotation will bring the points together with ellipses into the original position. The ellipse (95% reliability) is characterized by its area and the ratio of SEEL to SEET. Using voltammetric data the CE method has been applied to electrochemical analysis of the d(GCGAAGC) hairpin [44]. Confidence ellipses were calculated in MATLAB 6.5 program. The supplement program OUTLY was used for the elimination of points outside CE.

2.4.3 Medusa

The program MEDUSA (Make Equilibrium Diagrams Using Sophisticated Algorithms) was used for the construction of a distribution diagram of different Cu chemical forms present in corresponding electrolytes. The basic parameters, including equilibrium constants that are necessary for the calculation of distribution diagrams are in the program database. The program author is Ignasi Puigdomenech from the Inorganic Chemistry of Royal Institute of Technology, Stockholm, Sweden. The MEDUSA program is the free ware and is available on <http://www.kemi.kth.se/medusa>.

3. Results and Discussion

3.1. Electrode process of copper ions on PIGE

For this study, Cu(II) ions and their complexes with purine were evaluated on paraffin-impregnated graphite electrodes (PIGE) and effects of pH, the type and concentration of supporting electrolyte, the polarization rate, and accumulation parameters were tested. Cyclic voltammograms with reduction and oxidation Cu signals were recorded in the potential window from -1.0 to 1.0 V vs. Ag/AgCl/3M KCl. Whereas cyclic voltammograms of CuSO₄ in sulphate electrolytes showed only one anodic and one cathodic signal, CuCl₂ in chloride electrolytes gave two reduction (c₁, c₂) and two oxidation signals (a₁, a₂) (Figure 1). The values of peak potentials were strongly dependent on Cu(II) and chloride concentrations, scan rate, and pH. It is noteworthy that the behavior of Cu(II) with chloride as a supporting electrolyte was similar to that with bromide. According to chemical distribution diagrams constructed by MEDUSA program, Cu(II) signals on PIGE are strongly affected by Cu-halogen complexes. The pH and the CuX₂ concentration were the most important parameters. The separation of cathodic and anodic peaks can be caused by a specific catalytic effect of halogenide anions X⁻ (chlorides and bromides), which consists in the stronger attraction of positive charged species such as Cu(II), CuX(I) from solutions on the one hand and on the displacement of X⁻ from an electrode surface on the other [16,47]. Within the range from 0.01 mM to 1 mM CuCl₂, the dependences of peak heights on concentration were linear for cathodic and anodic signals. The pH dependence showed that alkaline solutions (pH > 8) did not encourage the formation of CV signals. This fact was supported by the distribution diagram MEDUSA which predicted lower concentrations of Cu(II) and/or CuX(I) due to

the formation of hydroxo-complexes. Moreover, above pH 8, the hydrolysis with the formation of $\text{CuO}\cdot\text{H}_2\text{O}$ takes place. The effect of pH on the separation of redox Cu peaks on vitreous carbon electrode was previously described [48].

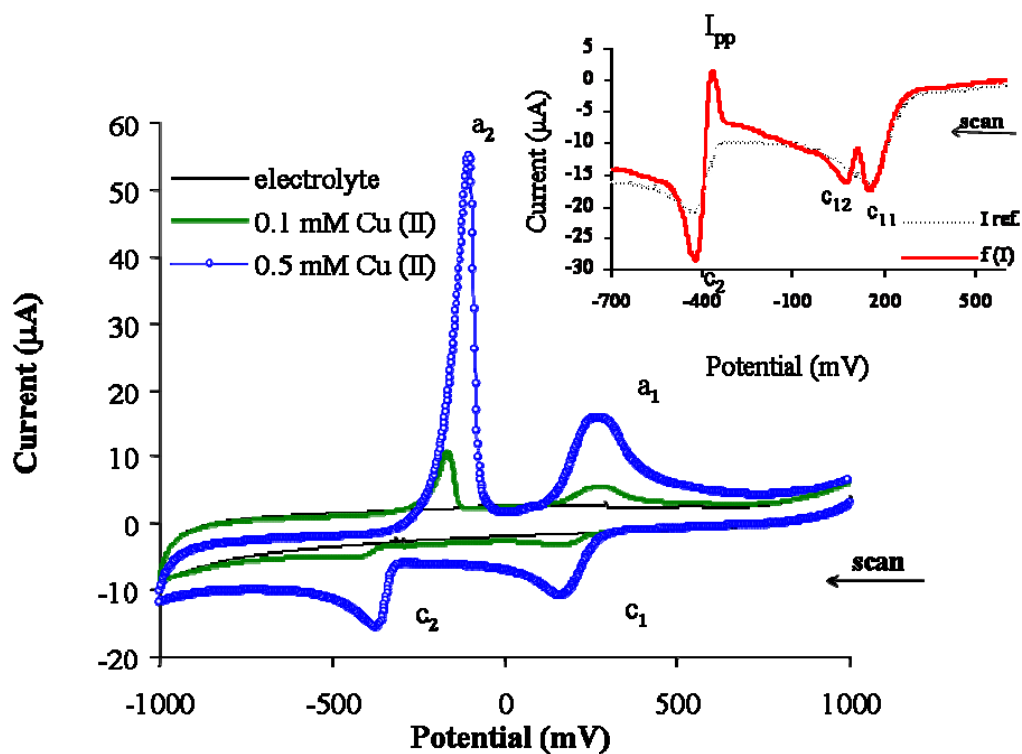


Figure 1. Cyclic voltammograms of 0.1 mM and 0.5 mM CuCl_2 on PIGE, scan rate 50 mV/s, c_1 and c_2 and a_1 and a_2 are cathodic and anodic signals, respectively. Supporting electrolyte was 0.5 M NaCl. Insert: LSV (I_{ref}) and corresponding EVLS curve $f(I)$ of Cu (II) reduction of 0.5 mM CuCl_2 , reference scan rate 100 mV/s. The I_{pp} is EVLS pre-peak, c_{11} and c_{12} are EVLS signals of c_1 . Voltammetric measurements were performed at a scan rate of 100 mV/s, starting potential 1 V, accumulation time 60 s, pH 6.0, and room temperature (25°C). For the EVLS procedure, scan rates of 50, 100, and 200 mV/s were used.

Excellent resolution of cathodic and anodic signals was observed in chlorides, and therefore the following experiments were carried out in this electrolyte. The apparent effect of scan rate on peak heights was used to find the rate determining step (*rds*) of the individual processes. For the first cathodic (c_1) and its corresponding anodic process (a_1), the scan rate exponent (0.47 and 0.48) revealed that both processes are controlled by diffusion. For the second redox processes, the exponents 0.28 and 0.35 for c_2 and a_2 , respectively, indicated the processes in which kinetics take place. For deeper insight into these processes the EVLS was utilized. The application of the elimination function E4 (Eq. 2), which eliminates simultaneously I_c and I_k with conserved I_d , for the cathodic processes is shown in the insert in Figure 1. Experiments were performed at scan rates of 50, 100, and 200 mV/s; the reference scan rate was 100 mV/s.

The elimination procedure divided c_1 signal into two peaks (c_{11} and c_{12}). The EVLS signal for c_2 showed a pre-peak which passed into higher peak than original one. It was found that peaks c_{11} and c_{12} were dependent on scan rates and Cu(II) concentrations. We propose that peak I corresponds to the reduction of Cu(II) (i.e., $\text{Cu(II)} + e \rightarrow \text{Cu(I)}$). According to computer calculations the concentrations of Cu(I) as species CuCl_2^- , CuCl_3^{2-} , and $\text{Cu}_2\text{Cl}_4^{2-}$ are higher than Cu(II) and CuCl(s) concentrations [49]. It is supported by founding that Cu(II) species dominated at chloride concentrations below 1mM and that soluble Cu(I) species dominated at chloride concentrations above about 100 mM. The one-charged cuprum ions can undergo the disproportionation reaction: $2\text{Cu(I)} \rightarrow \text{Cu(II)} + \text{Cu(0)}$. The Cu(II) ions arising from the disproportionation can be reduced at more negative potentials than the reduction of Cu(II) diffusing from solution towards to electrode surface. The above-mentioned dependence on scan rates and Cu(II) concentrations supported this assumption because the increase of these parameters caused the absence of both divided signals c_{11} and c_{12} . Due to the pre-peak I_{pp} of the signal c_2 , we have to consider the presence of a reaction preceding the electron transfer. This reaction could be associated with the replacement of chloride anions specifically adsorbed on electrode surface by electroactive species such as Cu(II) and/or Cu(I). Similar behavior characterized by I_{pp} was also observed for cadmium and nickel in chloride solutions [14-17].

3.2. Electrode process of copper ions on Hg-PGEb

Cyclic voltammograms of CuSO_4 in 0.05 M borax (pH 9.2) on the Hg-modified carbon electrode (Hg-PGEb) were measured in the potential range from -0.4 V to 0.1 V. Experimental conditions, including the preparation of the Hg-modified carbon electrode Hg-PGEb, were as described in previously published papers [3,4,50-52]. We found that the stabilization of electrode system was reached by the fifth cycle. Voltammetric curves obtained under these conditions are shown in Fig. 2. The cathodic peak c corresponds to the reduction process $\text{Cu(II)} + e^- \rightarrow \text{Cu(I)}$, including the above-mentioned disproportionation. The reduced Cu(0) is able to form an amalgam with Hg, which dissolves anodically (peak a). The differences between cathodic and anodic peak potentials were 73 and 208 mV for scan rates of 25 and 800 mV/s, respectively. The effect of thickness (138 nm, 275 nm, and 550 nm) of Hg-film on the peak height is shown in the insert in Fig. 2. The bilogarithmic dependence of current density j on scan rate, $\log j_c = f(\log \nu)$, yielded a slope of 0.78, suggesting a process controlled by diffusion but influenced by adsorption/desorption processes on the electrode surface. The Figs. 2B and C represent results of application of elimination function E4. Due to peak-counterpeak signals for lower scan rates (Fig. 2B), E4 signalized the reduction process of Cu in adsorption state [38,39,41]. For higher scan rates (Fig. 2C) the effect of adsorption is not obvious. The elimination procedure enhanced the signal more than nine times for both scan rate ranges compared to CV alone.

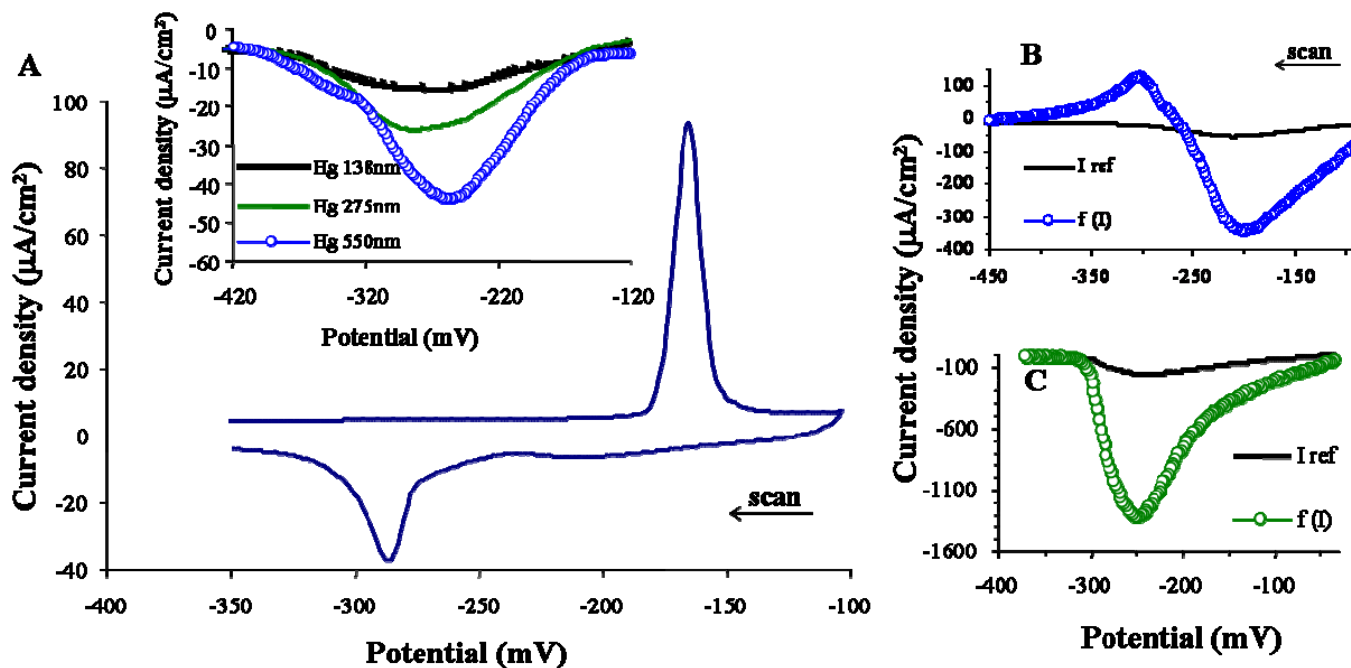


Figure 2. Voltammograms of 15 μM CuSO_4 in 0.05 M borax on Hg-PGEb at pH 9.2. (A) Cyclic voltammogram of 15 μM CuSO_4 in 0.05 M borax on Hg-PGEb, scan rate 25 mV/s, thickness of Hg layer 275 nm. Insert: cathodic peaks of 15 μM CuSO_4 with different Hg layer thicknesses (138 nm, 275 nm, and 550 nm). (B) Linear sweep voltammograms (I_{ref}) and elimination voltammograms (EVLS) for scan rates of 50, 100, and 200 mV/s, reference scan rate 100 mV/s., (C) Linear sweep voltammograms (I_{ref}) and elimination voltammograms (EVLS) for scan rates of 200, 400, and 800 mV/s, reference scan rate 400 mV/s.

3.3. Detection of purine-copper complexes on PIGE and Hg-PGEb

The change of cathodic and anodic signals of Cu(II) in NaCl on PIGE electrode after addition of adenine (Ade) is shown in Fig. 3. With increasing Ade concentration, the second cathodic signal (c_2) gradually disappeared, the second anodic peak (a_2) decreased, and the first anodic peak (a_1) increased (Fig. 3A). The distribution diagram (MEDUSA) revealed two Cu-Ade complexes containing cuprous Cu(Ade) and/or cupric ions Cu(Ade)₂ with ratios dependent on concentrations of copper ions and ligands. Under our experimental conditions, Cu(Ade) concentrations exceeded Cu(Ade)₂ concentrations by at least two orders of magnitude. As in experiments in the absence of Ade (samples containing only copper ions), the EVLS revealed important information about electrode processes. The function E4 detected two processes in the first peak c_1 (c_{11} and c_{12} in Fig. 3B) and also a change in the peak c_2 with the addition of Ade. While the process c_{11} corresponds to the Cu(II) reduction to Cu(I) at electrode surface, the process c_{12} represents the reduction of Cu(II) arising from the disproportionation step. We assume that the decrease of signal c_{12} upon addition of Ade is due to embedding of partially reduced Cu(II) into a copper-Ade complex. This idea is supported by fact that the peak c_{12} also decreased with increasing Cu concentration.

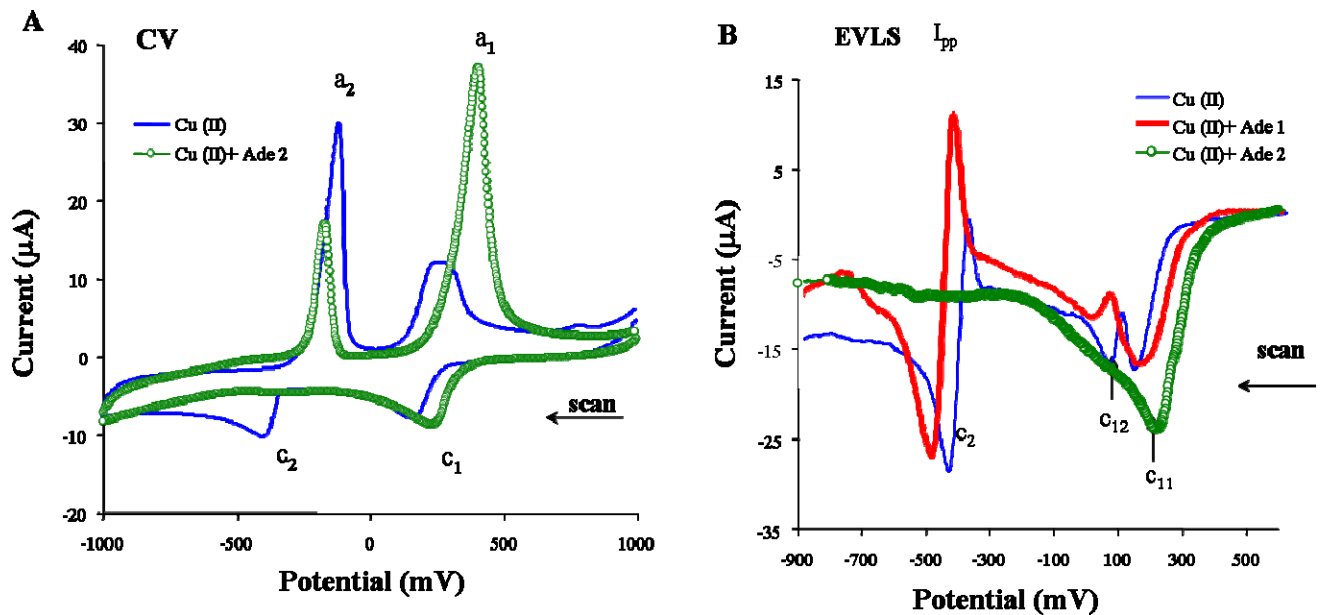


Figure 3. (A) Cyclic voltammograms of CuCl_2 with and without adenine on PIGE, scan rate 25mV/s, pH 6. (B) EVLS signals of cathodic processes of 0.5 mM CuCl_2 and CuCl_2 with adenine (Ade 1: 70 μM , Ade 2: 280 μM); reference scan rate 100 mV/s, pH 6.

For the detection of Cu-purine complex on PIGE, anodic stripping voltammetry (ASV) can be used. The accumulation potential (-50 mV) and accumulation time (60 s) were chosen to monitor the formation of the Cu-purine complex. The ASV and corresponding EVLS signals for adenine and guanine are shown in Fig. 4A and 4B, respectively. It is clear from our results that adenine provides higher ASV and EVLS signals than guanine. Moreover EVLS detected two ASV responses which will be described elsewhere. Hason et al. found that Hg-modified graphite/carbon electrodes are suitable for sensitive electrochemical detection of acid-treated (hydrolyzed) DNA (hODN) in the presence of the copper ions [4]. The procedure is based on the cathodic stripping of the electrochemically accumulated hODN-Cu(I) complex from the thin-film mercury modified graphite/carbon electrode surface. Whereas Cu-purine complexes on PIGE were detected by the anodic stripping technique, the detection of Cu-purine complexes on Hg-PGEb was carried out by means of cathodic stripping technique. The LSV (I_{ref}) and EVLS curves are shown in Fig. 4C and 4D for adenine and guanine, respectively. It was found that EVLS signals of both purines were increased relative to LSV: the amplification was 2.5 fold for Ade and 1.5 fold for Gua using PIGE and 17.2 fold for Ade and 11.1 fold for Gua using Hg-PGEb. Using EVLS we observed: a) higher CSV and corresponding EVLS signals than ASV signals, b) higher signals for adenine than guanine at both electrodes, and c) different E4 signals for adenine and guanine. In the case of ASV, the elimination procedure increased the corresponding signals (Fig. 4A and B), mainly due to responses at more positive potentials, but in the case of CSV this procedure yielded not only more sensitive, but totally different signals for adenine and guanine (Fig. 4C and D). The differences in the EVLS signals between ASV and CSV are probably related to different behaviors of Cu-Ade and Cu-Gua on Hg-film. Based on the existence of the peak-counterpeak EVLS signal, we assume that an adsorption of Cu-Gua takes place before its stripping.

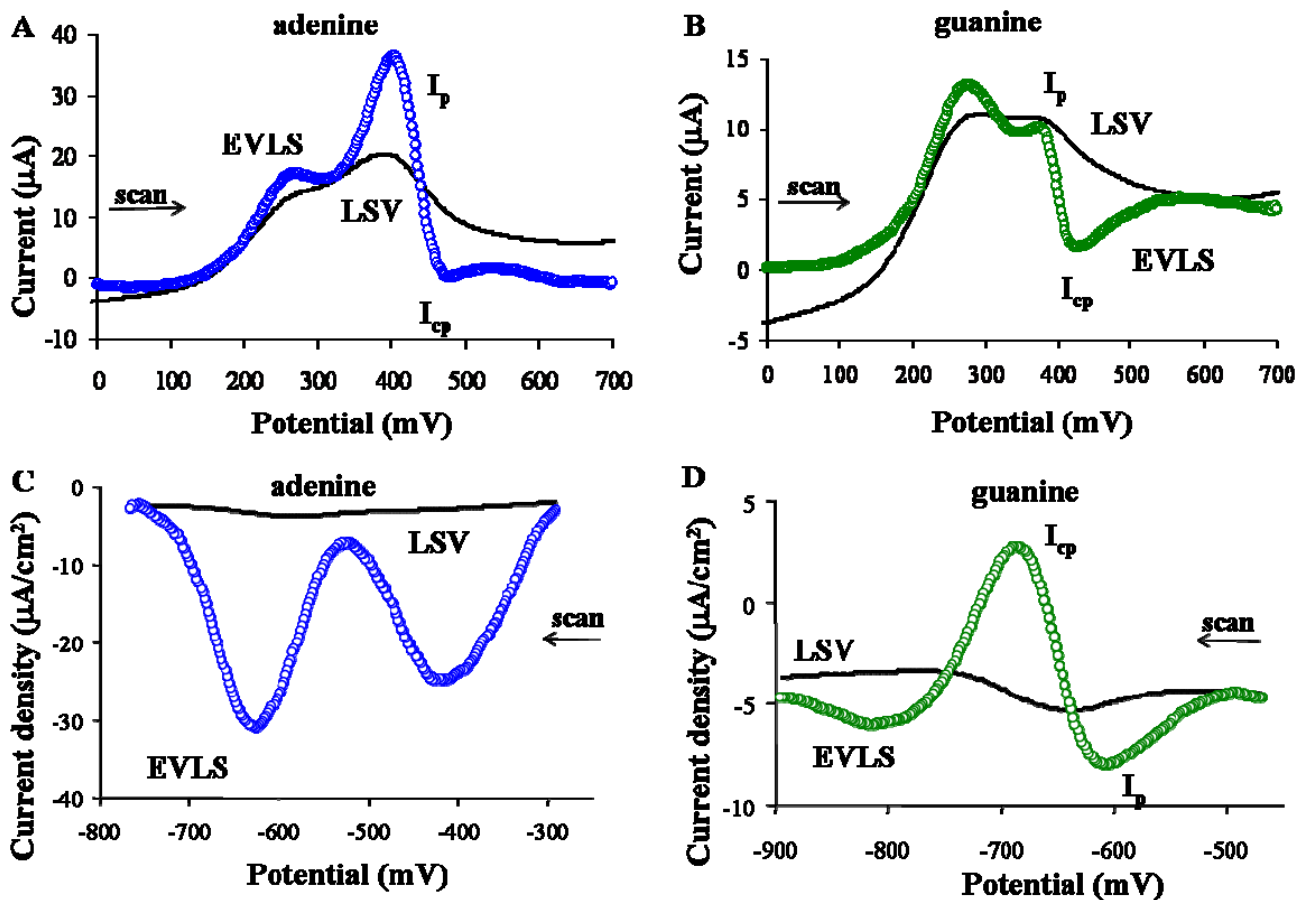


Figure 4. A) and B) Anodic stripping voltammograms on PIGE; time of accumulation 60 s, potential of accumulation -50 mV, pH 6. (A) LSV and EVLS curves of CuCl_2 with adenine; (B) LSV and EVLS curves of CuCl_2 with guanine, scan rate 100mV/s. (C) and (D) Cathodic stripping voltammograms on Hg-PGEb; time of accumulation 60 s, potential of accumulation -256 mV, pH 9.2. (C) LSV and EVLS curves of CuSO_4 with adenine, scan rate 200 mV/s; (D) LSV and EVLS curves of CuSO_4 with guanine, scan rate 50 mV/s.

3.4. Statistical evaluation of experiments on PIGE and Hg-PGEb

To obtain confidence ellipses [46,53], twelve samples of $10 \mu\text{M}$ CuCl_2 in 0.5M NaCl (pH 6) on PIGE at a scan rate of 100 mV/s (Fig. 5A) and twelve samples of $15 \mu\text{M}$ CuSO_4 in 0.05 M borax on Hg-PGEb (pH 9.2; thickness of Hg layer, 275nm) at a scan rate of 400 mV/s were measured (Fig. 5B). Confidence ellipses (CEs) with 95% reliability, including the ratio of the shorter to larger axis (b/a) and the area, were calculated by MATLAB 6.5 program. The first Fourier coefficients after the transformation of the curves are visualized by the points surrounded by CE. The CEs for both systems were characterized by the ratio $b/a = 0.116$ with an area of 0.009 (Fig. 5A) for PIGE and $b/a=0.026$ with an area of 1.745 for Hg-PGEb (Fig. 5B). These parameters indicate some deterministic effect in the repeated measurements of chosen CuCl_2 electrolyte. Higher ratio and lower surface (PIGE) indicate a lower systematic error; lower ratio and higher surface (Hg-PGEb) a higher systematic error. In Fig. 5A, points 1, 11, and 12 are out of the 95% CE and were eliminated using the OUTLY program

(written in MATLAB). After the elimination of these points, we obtained a ratio $b/a = 0.088$ with the area of 0.002 for PIGE.

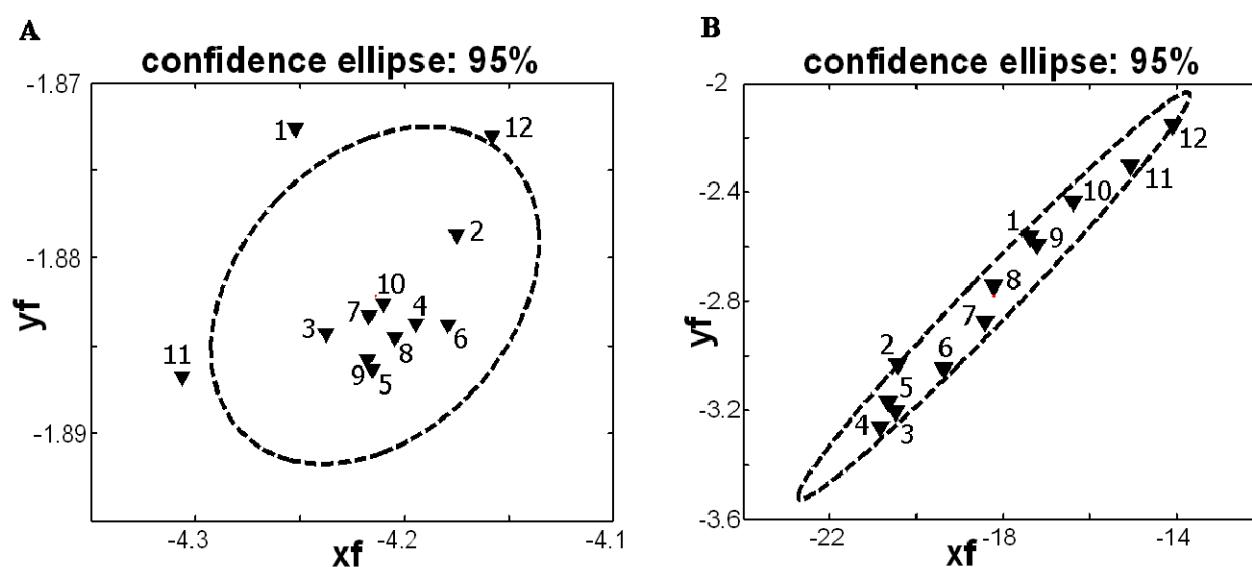


Figure 5. Confidence ellipses of Cu(II) (A) on PIGE (10 μM CuCl_2 in 0.5 M NaCl, pH 6, scan rate 100 mV/s), (B) on Hg-PGEb (thickness of Hg layer 275 nm, 15 μM CuSO_4 in 0.05 M borax, pH 9.2, scan rate 400 mV/s).

4. Conclusion

Our study of redox systems of Cu(II) on two modified graphite electrodes (PIGE and Hg-PGEb) in the presence or absence of purines contributes to the family of papers that deals with microdetection of purine bases and/or bases released from oligonucleotide chains by means of acid hydrolysis [3,7,26-28,50-52,54,55]. Deeper understanding of individual electrochemical steps in the Cu(II) reduction and higher sensitivity of Cu-purine detection was achieved by the application of EVLS to voltammetric curves. On the basis of the elimination function E4, we were able to distinguish between double-step and single-step reduction processes in the case of PIGE and Hg-PGEb, respectively. On PIGE, this EVLS function revealed reduction steps in which the formation of Cu(I), its disproportionation, and a surface reaction controlled by kinetics (e.g., adsorption/desorption, surface diffusion, nucleation) take place. Compared with PIGE, the surface of Hg-PGEb influences the reduction of Cu(II) such that the EVLS function E4 indicates the process in adsorption state. It was found that both stripping signals (i.e., ASV for PIGE and CSV for Hg-PGEb), indicated higher signals for the Cu-Ade complex than for the Cu-Gua complex. To evaluate the reproducibility of measurements, statistical data processing was carried out. Particularly, the confidence ellipses were plotted from twelve measurements for both electrode PIGE and Hg-PGEb. The systematic error was lower for PIGE than for Hg-PGEb.

The structure of Cu-purine complexes and the valence of Cu embedded in these complexes have been unclear. The formation of a Cu(I)-purine complex was supported by our EVLS results. We propose that (a) EVLS, in connection with the stripping procedure and optimal experimental conditions, can be useful tool offering quantitative and qualitative insight into the microanalysis of

purine derivatives, including structures of complexes and valences of metals, and (b) EVLS can be used to develop simple, fast, low-cost biosensors for the study of DNA hybridization and damage [56-59].

Acknowledgement

This work was supported by the grants INCHEMBIOL MSM0021622412, BIO-ANAL-MED LC06035, and COST OC174 from the Ministry of Education, Youth and Sports and by the grants A100040602 and A400040804 from the Grant Agency of the Academy of Sciences of the Czech Republic. The authors are indebted to Prof. M. Holik for discussion concerning confidence ellipses and to Mrs. I. Postbieglova for skillful technical assistance.

References

1. Palecek, E.; Jelen, F. *Electrochemistry of Nucleic Acids*; Elsevier: Amsterdam, 2005; pp. 74-173.
2. Fadrna, R.; Yosypchuk, B.; Fojta, M.; Navratil, T.; Novotny, L. Voltammetric determination of adenine, guanine, and DNA using liquid mercury free polished silver solid amalgam electrode. *Anal. Lett.* **2004**, *37*, 399-413.
3. Farias, P.A.M.; Wagener, A.D.; Castro, A.A. Ultratrace determination of adenine in the presence of copper by adsorptive stripping voltammetry. *Talanta* **2001**, *55*, 281-290.
4. Hason, S.; Jelen, F.; Fojt, L.; Vetterl, V. Determination of picogram quantities of oligodeoxynucleotides by stripping voltammetry at mercury modified graphite electrode surfaces. *J. Electroanal. Chem.* **2005**, *577*, 263-272.
5. Jelen, F.; Kourilova, A.; Pecinka, P.; Palecek, E. Microanalysis of DNA by stripping transfer voltammetry. *Bioelectrochemistry* **2004**, *63*, 249-252.
6. Wang, J.; Kawde, A.B. Amplified label-free electrical detection of DNA hybridization. *Analyst* **2002**, *127*, 383-386.
7. dosSantos, M.M.C.; Lopes, C.M.L.F.; Goncalves, M.L.S. Voltammetric studies of purine bases and purine nucleosides with copper. *Bioelectrochem. Bioenerg.* **1996**, *39*, 55-60.
8. Glodowski, S.; Bilewicz, R.; Kublik, Z. Determination of traces of purine by cathodic stripping voltammetry at the hanging copper amalgam drop. *Anal. Chim. Acta* **1986**, *186*, 39-47.
9. McCreery, R.L.; K., C.K. *Carbon Electrodes*, Marcel Dekker, 1996; 293-332.
10. Cui, H.; Zou, G.Z.; Lin, X.Q. Electrochemiluminescence of luminol in alkaline solution at a paraffin-impregnated graphite electrode. *Anal. Chem.* **2003**, *75*, 324-331.
11. Gong, J.M.; Lin, X.G. Facilitated electron transfer of hemoglobin embedded in nanosized Fe₃O₄ matrix based on paraffin impregnated graphite electrode and electrochemical catalysis for trichloroacetic acid. *Microchem. J.* **2003**, *75*, 51-57.
12. Komorsky-Lovric, S. Redox kinetics of adriamycin adsorbed on the surface of graphite and mercury electrodes. *Bioelectrochemistry* **2006**, *69*, 82-87.
13. Walcarius, A. Zeolite-modified paraffin-impregnated graphite electrode. *J. Solid State Electrochem.* **2006**, *10*, 469-478.

14. Orinakova, R.; Streckova, M.; Trnkova, L.; Rozik, R.; Galova, M. Comparison of chloride and sulphate electrolytes in nickel electrodeposition on a paraffin impregnated graphite electrode. *J. Electroanal. Chem.* **2006**, *594*, 152-159.
15. Orinakova, R.; Trnkova, L.; Galova, M.; Supicova, M. Application of elimination voltammetry in the study of electroplating processes on the graphite electrode. *Electrochim. Acta* **2004**, *49*, 3587-3594.
16. Rozik, R.; Trnkova, L. Cadmium reduction process on paraffin impregnated graphite electrode studied by elimination voltammetry with linear scan. *J. Electroanal. Chem.* **2006**, *593*, 247-257.
17. Streckova, M.; Orinakova, R.; Rozik, R.; Trnkova, L.; Galova, M. A study of nickel electrodeposition on paraffin-impregnated graphite electrode. *Helvetica Chim. Acta* **2006**, *89*, 622-634.
18. McCreery, R.L. *Electron Transfer Kinetics at Carbon Electrodes*; Marcel Dekker, 1991; pp. 221-374.
19. Dryhurst, G.; Elving, P.J. Electrochemical Oxidation of Adenine - Reaction Products and Mechanisms. *J. Electrochem. Soc.* **1968**, *115*, 1014-1020.
20. Goyal, R.N.; Brajtertoth, A.; Dryhurst, G. Further Insights into the Electrochemical Oxidation of Uric-Acid. *J. Electroanal. Chem.* **1982**, *131*, 181-202.
21. Goyal, R.N.; Rajeshwari, I.; Mathur, N.C. Electrochemical Oxidation of Uric-Acid and 6-Thiouric Acid. *Bioelectrochem. Bioenerg.* **1990**, *24*, 355-360.
22. Ibrahim, M.S.; Temerk, Y.M.; Kamal, M.M.; Ahmed, G.A.W.; Ibrahim, H.S.M. Ultra-sensitive anodic stripping voltammetry for the determination of xanthine at a glassy carbon electrode. *Microchim. Acta* **2004**, *144*, 249-256.
23. Kachoosangi, R.T.; Banks, C.E.; Compton, R.G. Simultaneous determination of uric acid and ascorbic acid using edge plane pyrolytic graphite electrodes. *Electroanalysis* **2006**, *18*, 741-747.
24. Shiraishi, H.; Takahashi, R. Accumulation of Adenine and Guanine as Cu⁺ Compounds at Glassy-Carbon Electrodes Followed by Anodic-Stripping Voltammetry. *Bioelectrochem. Bioenerg.* **1993**, *31*, 203-213.
25. Safavi, A.; Maleki, N.; Shams, E.; Shahbaazi, H.R. Determination of copper by adsorptive stripping voltammetry of its complex with adenine. *Electroanalysis* **2002**, *14*, 929-934.
26. Farias, P.A.M.; Wagener, A.D.R.; Bastos, M.B.R.; da Silva, A.T.; Castro, A.A. Cathodic adsorptive stripping voltammetric behaviour of guanine in the presence of copper at the static mercury drop electrode. *Talanta* **2003**, *61*, 829-835.
27. Farias, P.A.M.; Castro, A.A.; Wagener, A.D.R.; Junqueira, A.A. DNA determination in the presence of copper in diluted alkaline electrolyte by adsorptive stripping voltammetry at the mercury film electrode. *Electroanalysis* **2007**, *19*, 1207-1212.
28. Jelen, F.; Yosypchuk, B.; Kourilova, A.; Novotny, L.; Palecek, E. Label-Free Determination of Picogram Quantities of DNA by Stripping Voltammetry with Solid Copper Amalgam or Mercury Electrodes in the Presence of Copper. *Anal. Chem.* **2002**, *74*, 4788-4793.
29. Trnkova, L.; Dracka, O. Elimination voltammetry. Experimental verification and extension of theoretical results. *J. Electroanal. Chem.* **1996**, *413*, 123-129.

30. Palecek, E. Oszillographische Polarographie der Nucleinsäuren und ihrer Bestandteile. *Naturwiss.* **1958**, *45*, 186-187.
31. Trnkova, L.; Jelen, F.; Postbieglova, I. Application of elimination voltammetry to the resolution of adenine and cytosine signals in oligonucleotides. I. Homooligodeoxynucleotides dA(9) and dC(9). *Electroanalysis* **2003**, *15*, 1529-1535.
32. Trnkova, L.; Jelen, F.; Postbieglova, I. Application of elimination voltammetry to the resolution of adenine and cytosine signals in oligonucleotides II. Hetero-oligodeoxynucleotides with different sequences of adenine and cytosine nucleotides. *Electroanalysis* **2006**, *18*, 662-669.
33. Galus, Z. *Fundamentals of Electrochemical analysis*; Polish Scientific Publisher PWN, 1994.
34. Scholz, F. *Electroanalytical Methods, Guide to Experiment and Applications*; Springer: Heidelberg, Germany, 2002.
35. Scholz, F.; Meyer, B. Electrochemical solid state analysis: state of the art. *Chem. Soc. Rev.* **1994**, *23*, 341-347.
36. Dracka, O. Theory of current elimination in linear scan voltammetry. *J. Electroanal. Chem.* **1996**, *402*, 19-28.
37. Supicova, M.; Rozik, R.; Trnkova, L.; Orinakova, R.; Galova, M. Influence of boric acid on the electrochemical deposition of Ni. *J. Solid State Electrochem.* **2005**, *10*, 61-68.
38. Trnkova, L. Elektrochemické eliminační metody. *Chem. Listy* **2001**, *95*, 518-527.
39. Trnkova, L. Identification of current nature by elimination voltammetry with linear scan. *J. Electroanal. Chem.* **2005**, *582*, 258-266.
40. Trnkova, L.; Friml, J.; Dracka, O. Elimination voltammetry of adenine and cytosine mixtures. *Bioelectrochem.* **2001**, *54*, 131-136.
41. Trnkova, L.; Kizek, R.; Dracka, O. Application of elimination voltammetry to adsorptive stripping of DNA. *Electroanalysis* **2000**, *12*, 905-911.
42. Trnkova, L.; Kizek, R.; Dracka, O. Application of elimination methods in electrochemical study of DNA. *J. Biomol. Struct. Dynam.* **2000**, *17*, 1169-70.
43. Trnkova, L.; Kizek, R.; Dracka, O. Elimination voltammetry of nucleic acids on silver electrodes. *Bioelectrochem.* **2002**, *55*, 131-133.
44. Trnkova, L.; Postbieglova, I.; Holik, M. Electroanalytical determination of d(GCGAAGC) hairpin. *Bioelectrochem.* **2004**, *63*, 25-30.
45. Mikelova, R.; Trnkova, L.; Jelen, F.; Adam, V.; Kizek, R. Resolution of overlapped reduction signals in short hetero-oligonucleotides by elimination voltammetry. *Electroanalysis* **2007**, *19*, 348-355.
46. Holik, M.; Halamek, J. Transformation of a Free-Wilson Matrix into Fourier Coefficients. *Quant. Struct.-Act. Relat.* **2002**, *20*, 422-428.
47. Souto, R.M.; Saakes, M.; Sluyters-Rehbach, M.; Sluyters, J.H. The catalysis of the electrochemical reduction of cerium ions by chloride ions. *J. Electroanal. Chem.* **1988**, *245*, 167-189.
48. Grujicic, D.; Pesic, B. Reaction and nucleation mechanisms of copper electrodeposition from ammoniacal solutions on vitreous carbon. *Electrochim. Acta.* **2005**, *50*, 4426-4443.

49. Jagner, D.; Sahlin, E.; Renman, L. Experimental and Computational Study of Species Formed During Electrochemical Stripping Oxidation of Copper in Chloride Media - Determination of Copper(I) in the Ng 1(-1) Range by Stripping Potentiometry. *Talanta* **1995**, *42*, 1447-1455.
50. Hason, S.; Vetterl, V. Amplified oligonucleotide sensing in microliter volumes containing copper ions by solution streaming. *Anal. Chem.* **2006**, *78*, 5179-5183.
51. Hason, S.; Vetterl, V. Microanalysis of oligodeoxynucleotides by cathodic stripping voltammetry at amalgam-alloy surfaces in the presence of copper ions. *Talanta* **2006**, *69*, 572-580.
52. Jelen, F.; Hason, S.; Trnkova, L. *Microanalysis of nucleic acids bases and oligonucleotides by electrochemical stripping techniques*; Research Signpost, 2007; pp. 153-171.
53. Holik, M.; Halamek, J. Calculation of the tilts of curved lines. *Chemometrics Intell. Lab. Syst.* **2003**, *1382*, 1-9.
54. Bilewicz, R.; Glodowski, S.; Kublik, Z. The influence of adenine on the electrochemical behaviour of the Cu/II/ / Cu/0/ system. *J. Electroanal. Chem.* **1989**, *274*, 201-212.
55. Bilewicz, R.; Muszalska, E. Voltammetric behaviour of copper complexes with the antitumour drug 6-mercaptopurine. *J. Electroanal. Chem.* **1991**, *300*, 147-157.
56. Palecek, E.; Fojta, M. Detecting DNA hybridization and damage. *Anal. Chem.* **2001**, *73*, 74A-83A.
57. Thorp, H.H. Cutting out the middleman: DNA biosensors based on electrochemical oxidation. *Trends Biotechnol.* **1998**, *16*, 117-121.
58. Thorp, H.H. Reagentless detection of DNA sequences on chemically modified electrodes. *Trends Biotechnol.* **2003**, *21*, 522-524.
59. Wang, J. Towards genelectronics: Electrochemical biosensing of DNA hybridization. *Chem.-Eur. J.* **1999**, *5*, 1681-1685.